Amphiphilic Particles

DOI: 10.1002/anie.200803315

Nanoscale Tubular and Sheetlike Superstructures from Hierarchical Self-Assembly of Polymeric Janus Particles**

Lin Cheng, Guangzhao Zhang, Lei Zhu, Daoyong Chen,* and Ming Jiang*

Inspired by hierarchical protein self-assembly in biological systems, the self-assembly of nanoparticles into superstructures has attracted much attention because of potential applications of these superstructures in the fields such as electronic or optical materials and novel nanodevices.[1–5] Template-free self-assembly of nanoparticles with anisotropic interactions is of particular interest because it can lead to tailor-made complex superstructures.[1,6–8] In fact, Janus nanoparticles are nano-objects with anisotropic interactions.[9] The facile preparation, applications, and self-assembly of Janus nanoparticles have attracted extensive interest, and Janus particles with various sizes, structures, and compositions have been recently reported.[10–18] Several kinds of Janus particles are capable of self-assembling into regular superstructures. For example, Müller and co-workers reported that amphiphilic Janus micelles prepared from ABC triblock copolymers could self-assemble into spherical supermicelles.[19,20] Granick and co-workers reported that amphiphilic and zwitterionic Janus colloidal spheres could assemble in water to form ordered clusters.[21,22] In a recent study, we prepared Janus nanoparticles by using hybrid organic/inorganic nanotubes as a desymmetrization tool and the as-prepared amphiphilic Janus nanoparticles self-assembled into narrowly size-distributed flowerlike supermicelles in water.[23] Despite these results, assembly of Janus nanoparticles into superstructures other than spherical supermicelles or clusters, such as nanowires,[24] tubular and sheetlike superstructures, still remains challenging.

Herein, we report a novel mechanism for the formation of polymeric Janus particles from mixed-shell micelles (MSMs) and the template-free self-assembly of the Janus particles into tubular superstructures and nanosheets. Micelles with mixed P2VN/PEO shells were prepared by noncovalent cross-linking of poly(acrylic acid) (PAA) blocks by addition of 1,2-propanediamine (PDA) to a solution of PEO_{3500}-*b*-PAA_{3800}/$P2VN_{38000}$-*b*-PAA_{24000} (1:1 (w/w), PEO = poly(ethylene oxide), P2VN = poly(2-vinyl naphthalene), and the subscripts denote the molecular weights of the respective blocks) in DMF (Figure 1a). The molar ratio of AA/PDA was 1:5, and the total polymer concentration was 1.0 mg mL^{-1}.

MSMs with PEO/P2VN as the mixed shell and a PDA-cross-linked PAA network as the core were thus formed by noncovalent cross-linking. After switching the solvent from DMF to water (pH 7) by using dialysis, P2VN in the mixed shell collapsed into separated microdomains (Figure 1b). In water, P2VN microdomains were surrounded and protected by solvated PEO chains so that the MSMs were individually dispersed. By decreasing the pH value of the aqueous solution to 3.1, intramicellar complexation occurred between PEO and PAA (Figure 1c), which resulted in an asymmetric intramicellar phase separation between the PEO/PAA complex and P2VN. As a result, amphiphilic Janus nanoparticles with a hydrophobic P2VN domain (formed by aggregation of all the P2VN small domains in a MSM) on one side and a hydrophilic PEO/PAA complex domain on the opposite side were formed (Figure 1d). These Janus nanoparticles were able to self-assemble in water to produce tubular and sheetlike superstructures.

The average hydrodynamic radius, $\langle R_h \rangle$, of MSMs in DMF was 190 nm (Figure 2a, curve 1). In water, MSMs were individually dispersed with an $\langle R_h \rangle$ value of 140 nm (Figure 2a, curve 2) because of the protection of solvated PEO chains in the mixed shell. The decrease in the $\langle R_h \rangle$ value of the MSMs should result from the collapse of P2VN chains in water. In the transmission electron microscopy (TEM) image of MSMs cast from neutral water stained with RuO_4 (Figure 2b), contrast within each MSM was observed. The darker domains were assigned to P2VN microdomains (2–

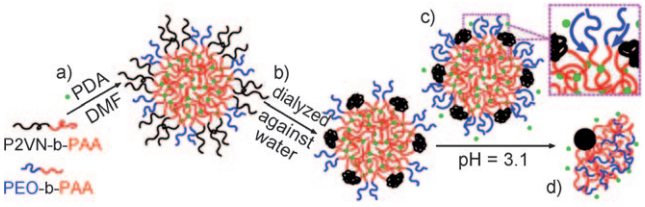

Figure 1. Schematic illustration of the processes for preparing MSMs in DMF (a) and in water (b), and the intramicelle complexation (c) to form Janus nanoparticles (d). Note that one MSM transforms into one Janus nanoparticle, and the black P2VN domain in the Janus nanoparticle was formed by aggregation of all the P2VN small domains in the MSM.

[*] L. Cheng, Prof. D. Chen, Prof. M. Jiang
The Key Laboratory of Molecular Engineering of Polymers and Department of Macromolecular Science, Fudan University
Shanghai, 200433 (P.R. China)
Fax: (+86) 21-6564-0293
Prof. G. Zhang
Department of Chemical Physics, University of Science and Technology of China, Hefei, Anhui, 230026 (P. R. China)
E-mail: chendy@fudan.edu.cn
Prof. L. Zhu
Institute of Materials Science and
Department of Chemical, Materials, and Biomolecular Engineering
University of Connecticut, Storrs, CT 06269 (USA)

[**] This work was supported by the NSFC (20528405, 20574014, 50825303, and 50773011), the Ministry of Science and Technology of China (2007CB936401 and 2009CB930400), and the Science and Technology Committee of Shanghai Municipality (07J14004).

Supporting information for this article is available on the WWW under http://dx.doi.org/10.1002/anie.200803315.

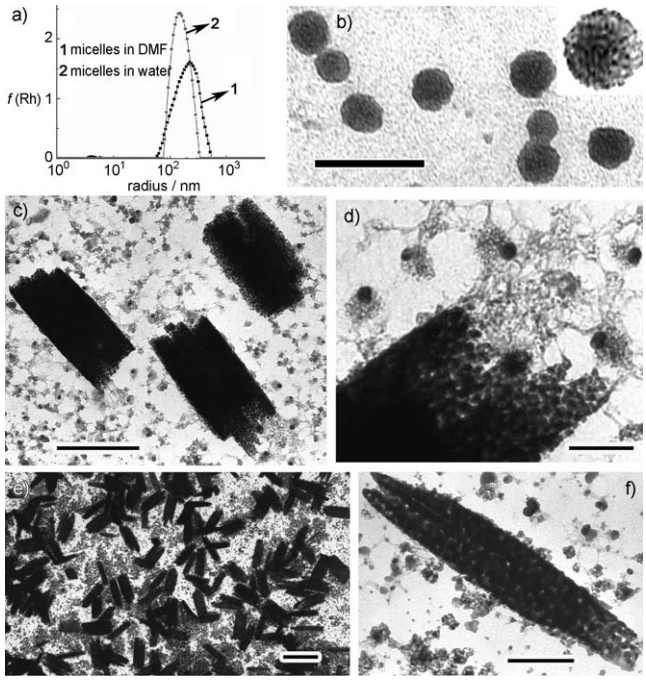

Figure 2. a) Hydrodynamic radius distributions of MSMs in DMF and water, respectively. b) TEM images of MSMs cast from water (stained with RuO_4). c) and d) TEM images of aggregates observed immediately after the pH reached 3.1 at different magnifications. e) and f) TEM images at different magnifications of aggregates observed for the precipitate that formed after 30 min. The scale bars are 100 nm (b), 500 nm (c), 100 nm (d), 1000 nm (e), and 200 nm (f).

3 nm). This morphology is consistent with what was expected for the mixed-shell micelles or particles.[25–27] The size of dried MSMs cast from water and observed by TEM was only 25–45 nm, which is much smaller than the $2\langle R_h\rangle$ value of MSMs in water (280 nm). This observation suggests that the PDA-cross-linked PAA core was highly swollen by water (see the Supporting Information) and was thus very flexible.

The pH value of the aqueous MSM solution was gradually lowered to induce PEO/PAA complexation. When the pH value of the solution was higher than 3.1, no aggregation among MSMs was detected by dynamic light scattering (DLS). At pH 3.1, the $\langle R_h\rangle$ value of MSMs increased rapidly with much stronger light scattering, which indicated the onset of aggregation or self-assembly among primary micelles (the hydrodynamic radius distributions of the aggregates formed at 5, 10, and 15 min after the pH reached 3.1 are presented in Figure S5 in the Supporting Information). The morphology of these aggregates was observed immediately by TEM and SEM (see the Supporting Information). Numerous Janus nanoparticles coexisting with rodlike aggregates were observed (Figure 2d and Figure S3 in the Supporting Information). The dried Janus nanoparticles had an average size of about 50 nm, being slightly larger than that of the MSMs cast from water in Figure 2b; the average length and width of the rodlike aggregates were 0.7 and 0.34 μm, respectively (Figure 2c and Figure S3 A in the Supporting Information). In the TEM images of the rodlike aggregates at high magnifications (Figure 2d, f), the nanorods were seen to be constructed from small particles, which were presumably the Janus nanoparticles. Furthermore, the morphology at the ends of the rodlike aggregates in the TEM and SEM images shows that the nanorods actually have a tubular superstructure (Figure 2d and Figures S3 and S4 in the Supporting Information).

Thirty minutes after the pH value reached 3.1, precipitates began to appear in the solution. TEM observations showed that the precipitates comprised nanotubules that were 0.85–1.1 μm in length and 0.2–0.4 μm in width (Figure 2e). The contrast observed within the nano-object in Figure 2f also demonstrated that it was constructed from small particles, and that it had a hollow interior (that is, a tubular superstructure) since solid nanorods with a diameter of 200–400 nm should not show such contrast in TEM.

After the precipitate was suspended in aqueous HCl (pH 3.1) with gentle magnetic stirring for one or two weeks, it was taken out of the suspension and then studied by TEM. The nanotubular morphology was the same as that of the freshly prepared sample. However, after gentle ultrasonication of the aqueous suspension of the precipitates (either freshly prepared or after standing for one or two weeks) for 20 seconds, nanosheets with a roughly trapezoidal shape were observed (Figure 3a) and most of the tubular superstructures disappeared. Furthermore, after a longer ultrasonication period (30 min or more) of the aqueous suspension containing the nanotubules, semicircular nanosheets were observed (Figure 3b, d and Figure S6 in the Supporting Information). AFM characterization of a completely dried nanosheet in Figure 3c showed that its average thickness was 29 nm, which is slightly larger than the average diameter of P2VN cores (ca. 20 nm, see Figure 2d). The outlines of individual dark P2VN particles were discernible in TEM images of the nanosheets at high magnifications (Figure 3d). Both AFM and TEM results suggested that the nanosheets consisted of a single layer of Janus nanoparticles, a tentative structure of the nanosheets is shown in the inset of Figure 3b.

The formation of Janus nanoparticles is a result of predesigned intramicellar complexation between PEO and PAA and concurrent asymmetric phase separation between P2VN and PEO/PAA complexes within a single micelle. In aqueous HCl (pH 3.1), PDA molecules were quarternized by H^+ ions and were ejected from the PAA core (see the Supporting Information). It was shown that PEO/PAA complexation took place in water at pH 3.1 (see the Supporting Information), and that the PAA core did not dissociate because of the interchain hydrogen bonding between PAA chains (supported by the DLS characterization data presented in Figure S5 in the Supporting Information). As a result, the PEO collapsed towards the core to complex with the PAA (intramicellar complexation), which led to deprotection of the hydrophobic P2VN microdomains in a MSM from the aqueous solution. Because of the high flexibility of the MSM cores (see the Supporting Information) and strong hydrophobic interactions, as well as possible π–π stacking between the naphthalene rings, the P2VN microdomains in a MSM aggregated to induce asymmetric phase separation between P2VN and PEO/PAA complexes within a single MSM. This resulted in amphiphilic Janus nanoparticles with a larger hydrophobic P2VN domain (ca. 20 nm) on one side and a hydrophilic PAA/PEO complex on the opposite side.

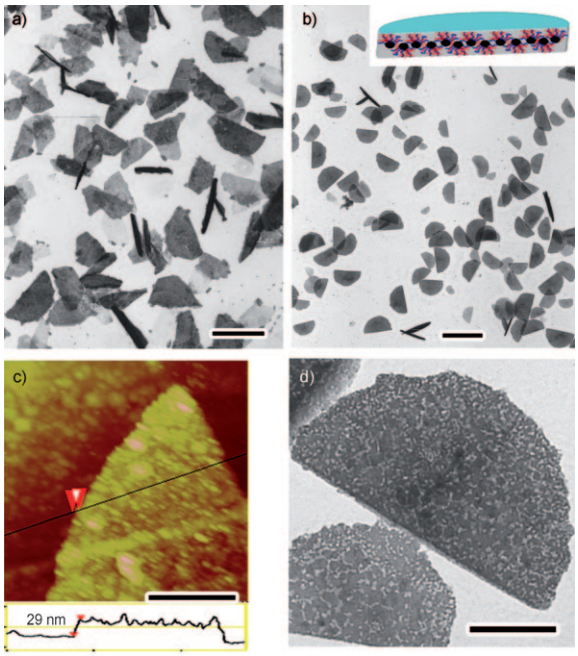

Figure 3. TEM images of the nanosheets with a trapezoidal shape (a) and a semicircular shape (b and d) after ultrasonication periods of 20 s (a) and 30 min or longer (b and d) of the nanotubules in aqueous solution (pH 3.1). The AFM image in (c) shows the thickness profile of the nanosheet. The scale bars in (a) and (b) are 1000 nm and the scale bars in (c) and (d) are 200 nm. The schematic representation of a nanosheet is shown in the inset of (b). P2VN microdomains are shown in black, PAA in red, and PEO in blue.

The diameter of dried MSMs observed by using TEM is about 25–45 nm; P2VN domains are clearly seen in relatively high contrast in the inset of Figure 2b. The P2VN domain size in a MSM is about 2–3 nm (some of the P2VN domains show a cylindrical morphology with a width of about 2–3 nm). In contrast, the P2VN domain in a Janus nanoparticle is about 20 nm (Figure 2d), which is much larger than the small P2VN domains in the MSMs. We infer that the intramicellar phase separation between P2VN and PEO/PAA complex at pH 3.1 led to the formation of Janus nanoparticles. During the formation of the Janus nanoparticles, all the 2–3 nm P2VN domains in a MSM aggregated together into one 20 nm P2VN domain to form the hydrophobic P2VN part (see the Supporting Information). However, in the tubular superstructures, the P2VN domains are approximately 15 nm, being a little smaller than but still comparable to the size of the P2VN domain in a Janus nanoparticle (the difference may result from the different states between the free Janus nanoparticles on carbon films and the Janus nanoparticles in the tubular superstructure). The average sizes of P2VN domains were measured by averaging over more than 30 P2VN domains in each case. Although the P2VN domains are partially fused together in the superstructures, we were able to differentiate some individual domains at high magnifications. The average sizes of the trapezoidal sheetlike superstructure (ca. 28 nm) and the semicircular sheetlike superstructure (ca. 40 nm) are much larger than P2VN domains in the tubular superstructure. The increase in the sizes of P2VN domains in the sheetlike superstructures might result from partial fusion of P2VN domains in the tubular structure under ultrasonication. The semicircular nanosheets were obtained by prolonged ultrasonication (30 min or longer). Therefore, P2VN domains fused more in the semicircular nanosheets than those in the trapezoidal nanosheets, as indicated by the further increase in the average size of P2VN domains in the semicircular sheetlike superstructure.

As mentioned above, the unique contrast seen in the tubular superstructures in the TEM images in Figure 2d,f indicates that they are constructed from small particles. At the early stage of self-assembly, Janus nanoparticles coexisted with nanotubes, whereas at the late stage (e.g., 30 min after the pH value reached 3.1), no Janus nanoparticles were observed. It is well known that lipid and rigid amphiphilic block copolymers are capable of forming layered structures with a relatively reduced curvature, such as vesicles and nanotubes, although the exact mechanism for the formation of tubules from lipids is still under debate. The amphiphilic Janus nanoparticles resemble lipid and rigid amphiphilic block copolymers in both structure and amphiphilicity. Therefore, it is reasonable for the amphiphilic Janus nanoparticles to form tubular and layered superstructures.[28–30] Therefore, we believe that the self-assembly of the amphiphilic Janus nanoparticles formed the tubular superstructure.

There are two possible pathways for the formation of nanosheets. The first is the dissociation of nanotubes into small particles that re-self-assemble into nanosheets. The second is the direct unwinding of nanotubes to form nanosheets. Given that the nanosheets were obtained after a very short (20 s) ultrasonication period (Figure 3a) and further ultrasonication led to even more regular nanosheets[16] (Figure 3b), the first pathway is thus unlikely. Besides, the trapezoidal and semicircular nanosheets are relatively uniform in shape and size, and their long dimensions are close to the average length of the tubular superstructures (see the Supporting Information). Therefore, we believe that the second pathway, that is, the unwinding of the nanotubes led to the formation of the nanosheets. The ultrasonication resulted in deformation or further fusion of the P2VN microdomains in the lateral direction, as shown by a larger average diameter of darker P2VN domains in the nanosheets in Figure 3d than those in Janus particles and nanotubes (Figure 2d,f). The fusion of P2VN microdomains could increase the bending rigidity of the layer, resulting in the unwinding and flattening of the nanotubes (see the Supporting Information). We speculate that further ultrasonication of the trapezoidal nanosheets could result in more regular shapes such as the semicircular nanosheets, because of rounding [16] of the obtuse angle corners in the trapezoidal nanosheets.

In conclusion, we have successfully prepared Janus nanoparticles from highly swollen MSMs based on a PDA cross-linked 1:1 (w/w) mixture of PEO-*b*-PAA and P2VN-*b*-PAA diblock copolymers in water. Lowering the pH value of the solution to 3.1 led to the intramicellar complexation between the PEO shell and the PAA core. Facilitated by the high flexibility and large mobility of the micelles, asymmetric intramicellar phase separation within a single micelle was induced to form Janus nanoparticles with hydrophobic P2VN on one side and a hydrophilic PEO/PAA complex on the

opposite side. Because of the amphiphilic nature of these Janus nanoparticles, they further self-assembled into tubular superstructures, which is reminiscent of the nanotubules formed by block copolymers and lipids. Upon ultrasonication, the tubular superstructure could unwind into trapezoidal (treatment for a short time) or semicircular (treatment for a long time) nanosheets. These novel superstructures from the self-assembly of amphiphilic Janus nanoparticles are promising candidates for nanodevices and sensors.

Experimental Section

Materials and instruments: $P2VN_{38000}$-*b*-PAA_{24000} was purchased from Polymer Source Inc. The subscripts indicate the molecular weights of the respective blocks. The molecular weight polydispersity index (PDI=M_w/M_n) of the block copolymer is 1.09. PEO_{3500}-*b*-PAA_{3800} was prepared and characterized according to the literature.[31–33] The PDI of PEO-*b*-PAA was 1.12. DMF (Shanghai Chemical Reagents Co.) of analytical purity was purified by reduced pressure distillation over CaH_2. 1,2-propanediamine (PDA, Aldrich) and hydrochloric acid (Shanghai Chemical Reagents Co.) of analytical purity were used without further purification.

Dynamic light scattering: A modified commercial light scattering spectrometer (ALV/SP-125) equipped with an ALV-5000 multi-τ digital time correlator and ADLAS DPY425 solid-state laser (output power = 22 mW at $\lambda = 632.8$ nm) was used. All the DLS measurements were performed at 90 and 25 °C.

Transmission electron microscopy: TEM observations were conducted on a Philips CM120 electron microscope at an acceleration voltage of 80 kV. Samples for TEM observations were prepared by depositing a drop of the aqueous suspensions onto a carbon-coated copper grid. Excess solution was absorbed using a filter paper.

Atomic force microscopy: AFM measurements were conducted on a Nanoscope III microscope (Digital Instruments). The samples were prepared by placing one drop of the aqueous suspension of the nanosheets on freshly cleaved mica and the excess solution was absorbed immediately using a filter paper.

Preparation of PEO/P2VN MSMs: In a typical procedure, P2VN-*b*-PAA (2 mg) and PEO-*b*-PAA (2 mg) were dissolved in distilled DMF (4 mL) and the solution stirred magnetically for 24 h. The molecular solubilization of the two block copolymers in DMF was confirmed by DLS measurements. Subsequently, PDA (9 mg) was added to the mixture and blue opalescence appeared instantaneously, which indicated the formation of aggregates in the solution. The resultant aggregate solution was stirred magnetically for 24 h before DLS measurements.

To switch the solvent from DMF to water, deionized water (0.5 mL) was added dropwise into a solution of MSMs in DMF (2 mL). No precipitate was observed. The solution was then dialyzed against deionized water for 1 day using a dialysis bag with a 14 kDa cut-off molecular weight. The total concentration of polymers in the resultant aqueous solution was approximately 0.5 mg mL^{-1}. The existence of PEO and PDA in the aqueous solution after the dialysis was confirmed by SEM energy dispersive X-ray (EDX) analysis and FTIR characterization (see the Supporting Information). This implies that the structure of the MSMs was preserved after dialysis (see the Supporting Information).

To assemble MSMs into tubular superstructure, aqueous HCl (1 M) was added dropwise to an aqueous suspension of the MSMs until the pH reached 3.1. To transform the tubular superstructure to trapezoidal and semicircular nanosheets, the aqueous suspension of the tubular superstructure was ultrasonicated for 20 s and 30 min, respectively, in an ultrasonic bath with an output power of 100 W.

Received: July 8, 2008
Revised: October 11, 2008
Published online: November 13, 2008

Keywords: amphiphiles · cross-linking · micelles · nanostructures · self-assembly

[1] Z. Zhang, Z. Tang, N. A. Kotov, S. C. Glotzer, *Nano Lett.* **2007**, *7*, 1670 – 1675.
[2] A. K. Boal, F. Ilhan, J. E. Derouchey, T. Thum-Albrecht, T. P. Russell, V. M. Rotello, *Nature* **2000**, *404*, 746 – 748.
[3] V. N. Manoharan, M. T. Elsesser, D. J. Pine, *Science* **2003**, *301*, 483 – 487.
[4] S. Y. Park, A. K. R. Lytton-Jean, B. Lee, S. Weigand, G. C. Schatz, C. A. Mirkin, *Nature* **2008**, *451*, 553 – 556.
[5] H. Duan, D. Wang, D. G. Kurth, H. Möhwald, *Angew. Chem.* **2004**, *116*, 5757 – 5760; *Angew. Chem. Int. Ed.* **2004**, *43*, 5639 – 5642.
[6] S. C. Glotzer, M. J. Solomon, *Nat. Mater.* **2007**, *6*, 557 – 562.
[7] Z. Tang, Z. Zhang, Y. Wang, S. C. Glotzer, N. A. Kotov, *Science* **2006**, *314*, 274 – 278.
[8] Z. Zhang, S. C. Glotzer, *Nano Lett.* **2004**, *4*, 1407 – 1413.
[9] Q. Sun, Q. Wang, P. Jena, Y. Kawazoe, *ACS Nano* **2008**, *2*, 341 – 347.
[10] C. J. Behrend, J. N. Anker, B. H. McNaughton, T. G. Roberts, M. Brasuel, M. A. Philbert, R. Kopelman, *J. Phys. Chem. B* **2004**, *108*, 10408 – 10414.
[11] M. Himmelhaus, H. Takei, *Sens. Actuators B* **2000**, *63*, 24 – 30.
[12] B. P. Binks, P. D. I. Fletcher, *Langmuir* **2001**, *17*, 4708 – 4710.
[13] H. Takei, N. Shimizu, *Langmuir* **1997**, *13*, 1865 – 1868.
[14] S. C. Glotzer, *Science* **2004**, *306*, 419 – 420.
[15] A. Perro, S. Reculusa, S. Ravaine, E. B. Bourgeat-Lami, E. Duguet, *J. Mater. Chem.* **2005**, *15*, 3745 – 3760.
[16] A. Walther, X. André, M. Drechsler, V. Abetz, A. H. E. Müller, *J. Am. Chem. Soc.* **2007**, *129*, 6187 – 6198.
[17] A. Walther, A. H. E. Müller, *Soft Matter* **2008**, *4*, 663 – 668.
[18] J. van Herrikhuyzen, G. Portale, J. C. Gielen, P. C. M. Christianen, N. A. J. M. Sommerdijk, S. C. J. Meskers, A. P. H. J. Schenning, *Chem. Commun.* **2008**, 697 – 699.
[19] R. Erhardt, A. Böker, H. Zettl, H. Kaya, W. Pyckhout-Hintzen, G. Krausch, V. Abetz, A. H. E. Müller, *Macromolecules* **2001**, *34*, 1069 – 1075.
[20] R. Erhardt, M. Zhang, A. Böker, H. Zettl, C. Abetz, P. Frederik, G. Krausch, V. Abetz, A. H. E. Müller, *J. Am. Chem. Soc.* **2003**, *125*, 3260 – 3267.
[21] L. Hong, A. Cacciuto, E. Luijten, S. Granick, *Langmuir* **2008**, *24*, 621 – 625.
[22] L. Hong, A. Cacciuto, E. Luijten, S. Granick, *Nano Lett.* **2006**, *6*, 2510 – 2514.
[23] L. Nie, S. Liu, W. Shen, D. Chen, M. Jiang, *Angew. Chem.* **2007**, *119*, 6437 – 6440; *Angew. Chem. Int. Ed.* **2007**, *46*, 6321 – 6324.
[24] E. R. Zubarev, J. Xu, A. Sayyad, I. D. Gibson, *J. Am. Chem. Soc.* **2006**, *128*, 15098 – 15099.
[25] T. Hui, D. Chen, M. Jiang, *Macromolecules* **2005**, *38*, 5834 – 5837.
[26] R. Zheng, G. Liu, X. Yan, *J. Am. Chem. Soc.* **2005**, *127*, 15358 – 15359.
[27] L. Zhu, B. Zhao, *J. Phys. Chem. B* **2008**, *112*, 11529 – 11536.
[28] J. Raez, J. P. Tomba, I. Manners, M. A. Winnik, *J. Am. Chem. Soc.* **2003**, *125*, 9546 – 9547.
[29] E. Lee, Y. H. Jeong, J. K. Kim, M. Lee, *Macromolecules* **2007**, *40*, 8355 – 8360.
[30] J. Kim, E. Lee, Y. Jeong, J. Lee, W. Zin, M. Lee, *J. Am. Chem. Soc.* **2007**, *129*, 6082 – 6083.
[31] M. Bednarek, T. Biedron, P. Kubisa, *Macromol. Rapid Commun.* **1999**, *20*, 59 – 65.
[32] S. Liu, J. V. M. Weaver, Y. Tang, N. C. Billingham, S. P. Armes, K. Tribe, *Macromolecules* **2002**, *35*, 6121 – 6131.
[33] C. Gu, D. Chen, M. Jiang, *Macromolecules* **2004**, *37*, 1666 – 1669.

